Electromagnetic Modeling of Wind Tunnel Magnetic Suspension and Balance Systems

Colin P. Britcher*
Old Dominion University, Norfolk, VA 23529, USA

Desiree Driver†
Leidos, Bridgewater, VA, 22812, USA

David E. Cox‡
NASA Langley Research Center, Hampton, VA 23666, USA

An analytical framework for the open-loop behavior of a permanent magnet element levitated within an applied magnetic field is shown in the context of application to wind tunnel Magnetic Suspension and Balance Systems (MSBS). Various modes of motion are identified, which correlate with observed behavior of the NASA/ODU 6-inch MSBS. This system is being developed as a technology demonstrator for dynamic stability testing of atmospheric entry capsules, with possible application to a supersonic wind tunnel. The analytic equations are populated with field information from experimental measurements and a finite element model. Finally, a system simulation can provide alternative estimates of system dynamic behavior via model linearization, with preliminary comparisons presented. Taken together, the analytical framework, experimental measurement, finite element analysis, and dynamic simulation provide a complete understanding of the characteristics and behavior of the MSBS.

I. Nomenclature

B	=	magnetic flux density (Tesla)
F	=	force (N)
I	=	moment of inertia
$K1$	=	field coefficients (T/A)
$K2$	=	field gradient coefficients (T/m/A)
m	=	mass
M	=	magnetization (A/m)
T	=	torque (Nm)
Vol	=	volume
ϕ, θ, ψ	=	roll, pitch, yaw

II. Introduction

Magnetic suspension provides a means to support a wind tunnel model without any interference to the flow from a sting or struts (Figure 1). It also allows more flexibility for tailoring the stiffness of that support, to both translational and rotational forces/torques, compared to a physical mount. This makes it a promising technology for characterization of planetary entry vehicle dynamics, as these vehicles typically have stability properties that depend on wake dynamics. This paper will address two aspects of the modeling of wind tunnel Magnetic Suspension and Balance

* Professor, Department of Mechanical and Aerospace Engineering, AIAA Associate Fellow.
† Project Manager, Formerly Graduate Research Assistant, ODU
‡ Senior Research Engineer, Dynamic Systems and Control Branch.

Systems (MSBS). First, a theoretical framework for the equations of motion of the suspended model, originally set out by Groom [4], will be adapted for the wind tunnel application with various possible directions of model magnetization. Second, a finite element model of the existing MSBS will be shown, together with experimental verification via field surveys.

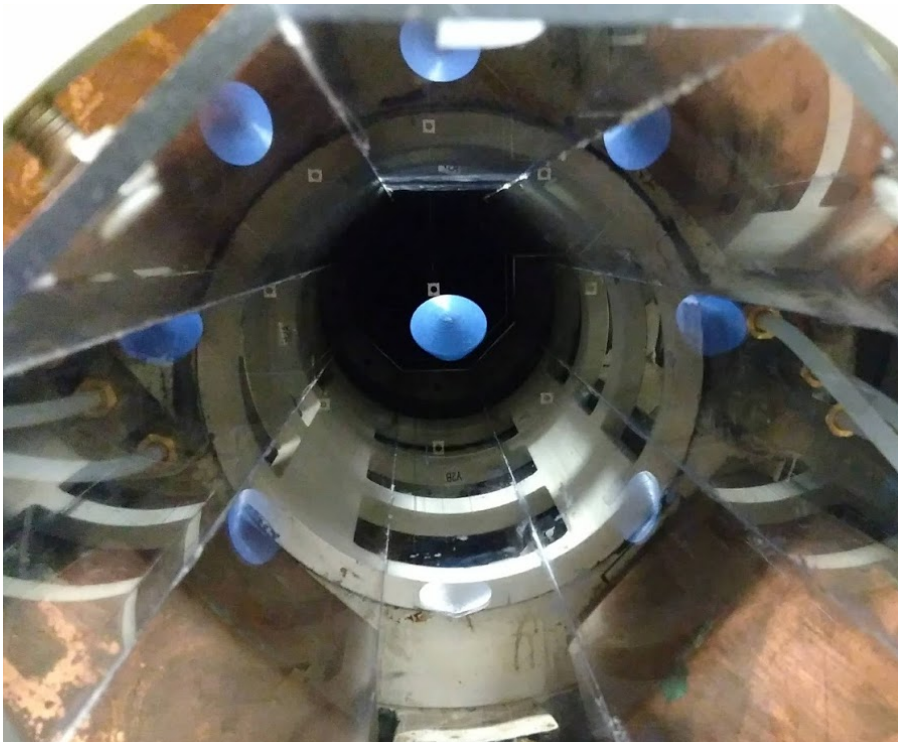

Fig. 1 The NASA/ODU 6-inch Magnetic Suspension and Balance System (Stardust capsule, centered in blue)

III. Equations of Motion of a Generic MSBS (with vertical magnetization)

The magnetization direction in MSBS applications was traditionally along the tunnel axis (i.e., x, see Figure 2). The NASA/ODU 6-inch MSBS has been reconfigured to operate with transverse magnetization, thereby developing a free-to-rotate axis for dynamic stability testing [2]. The following derivation proceeds with vertical magnetization (M_z) and can be repeated for the other principal magnetization directions (x, y), as outlined in the Appendix.

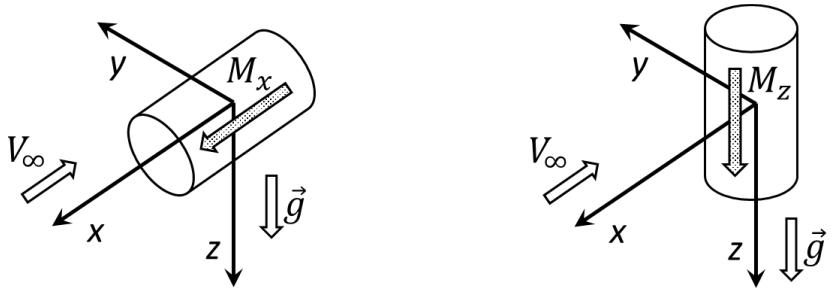

Fig. 2 Coordinate System and Magnetization Axis – axial (left) and vertical (right)

The governing equations for magnetic force and torque on a levitated object are:

(1)

$$\vec{F} = \iiint d\vec{M}.\nabla\vec{B} = \iiint (\vec{M}.\nabla\vec{B})dVol$$

$$\vec{T} = \iiint d\vec{M} \times \vec{B} = \iiint (\vec{M} \times \vec{B})dVol$$

If the magnetization of the magnetic core is considered uniform and aligned with the z axis (which is initially vertical in the wind tunnel coordinate system) then these reduce to:

$$\begin{gathered} F_x\ (\equiv \mathcal{X}) \approx Vol\ M_z B_{xz} \quad ; \quad F_y\ (\equiv \mathcal{Y}) \approx Vol\ M_z B_{yz} \quad ; \quad F_z\ (\equiv \mathcal{Z}) \approx Vol\ M_z B_{zz} \\ T_x\ (\equiv \mathcal{L}) \approx -Vol\ M_z B_y \quad ; \quad T_y\ (\equiv \mathcal{M}) \approx Vol\ M_z B_x \quad ; \quad T_z\ (\equiv \mathcal{N}) \approx 0 \end{gathered} \tag{2}$$

In Appendix-A modifications required for a horizontally magnetized core are developed. For a permanent magnet core, these equations may be sufficient. For the case of a freely magnetized iron core, additional equations will be necessary to determine the level of magnetization [3].

The magnetic fields and gradients created by the array of *n* external electromagnets can be related to electromagnet currents as follows, provided electromagnet core materials are operated in their linear ranges (below saturation):

$$\vec{B} = \begin{bmatrix} B_x \\ B_y \\ B_z \end{bmatrix} = \begin{bmatrix} K1_{x,1} & \cdots & K1_{x,n} \\ K1_{y,1} & \cdots & K1_{y,n} \\ K1_{z,1} & \cdots & K1_{z,n} \end{bmatrix} \begin{pmatrix} I_1 \\ \vdots \\ I_n \end{pmatrix} \quad ; \quad \partial\vec{B} = \begin{bmatrix} B_{xx} \\ B_{xy} \\ B_{xz} \\ B_{yy} \\ B_{yz} \end{bmatrix} \begin{bmatrix} K2_{xx,1} & \cdots & K2_{xx,n} \\ K2_{xy,1} & \cdots & K2_{xy,n} \\ K2_{xz,1} & \cdots & K2_{xz,n} \\ K2_{yy,1} & \cdots & K2_{yy,n} \\ K2_{yz,1} & \cdots & K2_{yz,n} \end{bmatrix} \begin{pmatrix} I_1 \\ \vdots \\ I_n \end{pmatrix} \tag{3}$$

As written here, there are 3 components of magnetic field and only 5 independent components of field gradients $(B_{xx} + B_{yy} + B_{zz} = 0)$, although the dependent term (B_{zz}) can be retained for convenience. The coefficients *K*1 and *K*2 can be calculated analytically for some simple air-cored coil shapes but are generally best estimated from finite element analysis.

Since controller design approaches typically rely on a comprehensive dynamic system model, a novel formulation of the open-loop equation of motion was developed by Groom et al [4, 5]. Here, this derivation will be adapted to the case of alternative orientations of the magnetization of the suspended element with application to MSBSs. Note that the reference literature addresses the particularly challenging case of levitation above a planar array of electromagnets by repulsion from below, which gives rise to strong instabilities.

Following Groom [4], the magnetization of the suspended element and the transformation between inertial (wind tunnel) axes and magnetic core coordinates are as follows (small angle approximations apply throughout):

$$\vec{M} = \begin{Bmatrix} 0 \\ 0 \\ M_z \end{Bmatrix} \quad ; \quad T_m = \begin{bmatrix} 1 & \psi & -\vartheta \\ -\psi & 1 & \emptyset \\ \vartheta & -\emptyset & 1 \end{bmatrix} \tag{4}$$

The forces and torques on the suspended element can be written as

$$\overrightarrow{F_c} = Vol\ [T_m] \begin{bmatrix} B_{xx} & B_{xy} & B_{xz} \\ B_{xy} & B_{yy} & B_{yz} \\ B_{xz} & B_{yz} & B_{zz} \end{bmatrix} [T_m]^{-1} \vec{M} \quad ; \quad \overrightarrow{T_c} = Vol\ \vec{M} \times [T_m]\vec{B} \tag{5}$$

These reduce to

$$\overrightarrow{F_c} \approx Vol\ M_z \begin{pmatrix} B_{xz} - B_{xy}\phi + (B_{xx} - B_{xx})\vartheta + B_{yz}\psi \\ B_{yz} - (B_{yy} - B_{zz})\phi + B_{xy}\vartheta - B_{xz}\psi \\ B_{zz} - 2B_{yz}\phi + 2B_{xz}\vartheta \end{pmatrix} \quad ; \quad \overrightarrow{T_c} \approx Vol\ M_{zx} \begin{pmatrix} -B_y - B_z\phi + B_x\psi \\ B_x - B_z\vartheta + B_y\psi \\ 0 \end{pmatrix} \tag{6}$$

The first terms in each right-hand-side matrix are the "primary" terms, as seen in the initial governing equations. The other terms represent various couplings between degrees of freedom and are discussed more fully below. Note that these only arise if the appropriate field or field gradient components are non-zero. B_z would be non-zero with a magnetized iron core, or with an axial field, so the associated terms in the torque equation ($B_z\phi$ and $B_z\vartheta$) correspond to the tendency of the magnetization vector to align with the applied field. They are consequently referred to as "compass needle" terms and can be non-zero if an axial alignment field is present or can be zero if rotations are

feedback controlled. By contrast, the coupling terms in the force matrix cannot all be made zero in meaningful applications since some non-zero field gradients will necessarily be present in order to generate magnetic forces.

It should also be noted that rotation about the model's magnetization axis (ψ here) is retained in this formulation since the model's geometric axis of symmetry will be orthogonal to the axis of magnetization in this newer MSBS configuration. In Groom's original work, the model was axisymmetric and axially magnetized with rotation about its own axis therefore considered unimportant.

Finally, the fact that the last row in the torque matrix is zero corresponds to the well-known fact that torque cannot be generated about the axis of magnetization, unless symmetry is broken; the classical "roll control" problem in MSBSs [6].

The equations are now recast in state-space form, using a full state vector, with an ordering revised from that originally used by Groom. Note also that the axis system used herein corresponds to conventional aircraft axes, with the z axis downwards (Fig. 2).

$$\boldsymbol{X} = (u \quad v \quad w \quad p \quad q \quad r \quad x \quad y \quad z \quad \phi \quad \vartheta \quad \psi)^T \tag{7}$$

$$(\dot{\boldsymbol{X}}) = [W1]\begin{bmatrix} \mathcal{Z} & \mathcal{Z} & \mathcal{FP} & \mathcal{FA} \\ \mathcal{Z} & \mathcal{Z} & \mathcal{TP} & \mathcal{TA} \\ \mathcal{I} & \mathcal{Z} & \mathcal{Z} & \mathcal{Z} \\ \mathcal{Z} & \mathcal{I} & \mathcal{Z} & \mathcal{Z} \end{bmatrix}(\boldsymbol{X}) + \begin{bmatrix} K2_{xz,1} & \cdots & K2_{xz,n} \\ K2_{yz,1} & \cdots & K2_{yz,n} \\ K2_{zz,1} & \cdots & K2_{zz,n} \\ -K1_{y,1} & \cdots & -K1_{y,n} \\ K1_{x,1} & \cdots & K1_{x,n} \\ 0 & \cdots & 0 \\ 0 & \cdots & 0 \\ 0 & \cdots & 0 \\ 0 & \cdots & 0 \\ 0 & \dots & 0 \\ 0 & \dots & 0 \\ 0 & \dots & 0 \end{bmatrix}\begin{pmatrix} I_1 \\ \vdots \\ I_n \end{pmatrix} \tag{8}$$

$$\mathcal{Z} = \begin{bmatrix} 0 & 0 & 0 \\ 0 & 0 & 0 \\ 0 & 0 & 0 \end{bmatrix} \quad ; \quad \mathcal{I} = \begin{bmatrix} 1 & 0 & 0 \\ 0 & 1 & 0 \\ 0 & 0 & 1 \end{bmatrix} \tag{9}$$

The force and torque derivative sub-matrices can be evaluated from the previous force equations:

$$\mathcal{FP} = \begin{bmatrix} X_x & X_y & X_z \\ Y_x & Y_y & Y_z \\ Z_x & Z_y & Z_z \end{bmatrix} = Vol\ M_x \begin{bmatrix} B_{xz}|_x & B_{xz}|_y & B_{xz}|_z \\ B_{yz}|_x & B_{yz}|_y & B_{yz}|_z \\ B_{zz}|_x & B_{zz}|_y & B_{zz}|_z \end{bmatrix} \tag{10}$$

$$\mathcal{FA} = \begin{bmatrix} X_\phi & X_\vartheta & X_\psi \\ Y_\phi & Y_\vartheta & Y_\psi \\ Z_\phi & Z_\vartheta & Z_\psi \end{bmatrix} = Vol\ M_x \begin{bmatrix} -B_{xy} & (B_{xx} - B_{zz}) & B_{yz} \\ (B_{zz} - B_{yy}) & B_{xy} & -B_{xz} \\ -2B_{yz} & 2B_{xz} & 0 \end{bmatrix} \tag{11}$$

$$\mathcal{TP} = \begin{bmatrix} \mathcal{L}_x & \mathcal{L}_y & \mathcal{L}_z \\ \mathcal{M}_x & \mathcal{M}_y & \mathcal{M}_z \\ \mathcal{N}_x & \mathcal{N}_y & \mathcal{N}_z \end{bmatrix} = Vol\ M_x \begin{bmatrix} -B_{xy} & -B_{yy} & -B_{yz} \\ B_{xx} & B_{xy} & B_{xz} \\ 0 & 0 & 0 \end{bmatrix} \tag{12}$$

$$\mathcal{TA} = \begin{bmatrix} \mathcal{L}_\phi & \mathcal{L}_\vartheta & \mathcal{L}_\psi \\ \mathcal{M}_\phi & \mathcal{M}_\vartheta & \mathcal{M}_\psi \\ \mathcal{N}_\phi & \mathcal{N}_\vartheta & \mathcal{N}_\psi \end{bmatrix} = Vol\ M_x \begin{bmatrix} -B_z & 0 & B_x \\ 0 & -B_z & B_y \\ 0 & 0 & 0 \end{bmatrix} \tag{13}$$

The matrix $\mathcal{W}1$ contains mass and inertia terms on the leading diagonal.

$$[W1] = \begin{bmatrix} \mathcal{M} & \mathcal{Z} & \mathcal{Z} & \mathcal{Z} \\ \mathcal{Z} & \mathcal{N} & \mathcal{Z} & \mathcal{Z} \\ \mathcal{Z} & \mathcal{Z} & \mathcal{I} & \mathcal{Z} \\ \mathcal{Z} & \mathcal{Z} & \mathcal{Z} & \mathcal{I} \end{bmatrix} \tag{14}$$

$$\mathcal{M} = \begin{bmatrix} {}^{1}/_{m} & 0 & 0 \\ 0 & {}^{1}/_{m} & 0 \\ 0 & 0 & {}^{1}/_{m} \end{bmatrix} \quad ; \quad \mathcal{N} = \begin{bmatrix} {}^{1}/_{I_x} & 0 & 0 \\ 0 & {}^{1}/_{I_y} & 0 \\ 0 & 0 & {}^{1}/_{I_z} \end{bmatrix} \tag{15}$$

The gradient components previously identified as primary (B_{xz}, B_{yz}, B_{zz}) are non-zero in the presence of external forces. Considering gravitational as well as aerodynamic lift, side, and drag forces:

$$(F_x)_{external} = -D \quad ; \quad \left(F_y\right)_{external} = S \quad ; \quad (F_z)_{external} = -L + m_c g \tag{16}$$

In equilibrium:

$$F_x = -(F_x)_{external} \quad ; \quad F_y = -\left(F_y\right)_{external} \quad ; \quad F_z = -(F_z)_{external} \tag{17}$$

$$\therefore \ \overline{B_{xz}} = \frac{D}{Vol\, M_z} \quad ; \quad \overline{B_{yz}} = \frac{-S}{Vol\, M_x} \quad ; \quad \overline{B_{zz}} = \frac{L - m_c g}{Vol\, M_z} \tag{18}$$

These terms must now be mapped into magnetic core coordinates using the same procedures as before. The $\mathcal{FA}$ matrix is augmented as follows:

$$\mathcal{FA}' = \begin{bmatrix} X_\phi & X_\vartheta & X_\psi \\ Y_\phi & Y_\vartheta & Y_\psi \\ Z_\phi & Z_\vartheta & Z_\psi \end{bmatrix} = Vol\, M_x \begin{bmatrix} -B_{xy} & (B_{xx} - B_{zz}) & B_{yz} \\ (B_{zz} - B_{yy}) & B_{xy} & -B_{xz} \\ -2B_{yz} & 2B_{xz} & 0 \end{bmatrix} + \begin{bmatrix} 0 & -(L - m_c g) & -S \\ L - m_c g & 0 & -D \\ S & D & 0 \end{bmatrix} \tag{19}$$

The ***A*** matrix can now be populated, and eigenvalues/eigenvectors derived, which describe the open-loop natural modes.

$$\boldsymbol{A} = [W1] \begin{bmatrix} \mathcal{Z} & \mathcal{Z} & \mathcal{FP} & \mathcal{FA}' \\ \mathcal{Z} & \mathcal{Z} & \mathcal{TP} & \mathcal{TA} \\ \mathcal{I} & \mathcal{Z} & \mathcal{Z} & \mathcal{Z} \\ \mathcal{Z} & \mathcal{I} & \mathcal{Z} & \mathcal{Z} \end{bmatrix} \tag{20}$$

IV. Finite Element Modeling of the NASA/ODU 6-Inch MSBS

The configuration of the NASA/ODU 6-inch MSBS is summarized in Figure 3. As currently configured, four sets of coils are independently powered to generate a vertical force (via the "Helmholtz" coil pair, B_{zz}), side force (via the

"Saddle" coils, B_{yz}) and a combined drag and vertical alignment field (via the front and rear "Lift" coil pairs, B_{xz} and B_z). This utilization of coils differs considerably from the original MIT configuration [7].

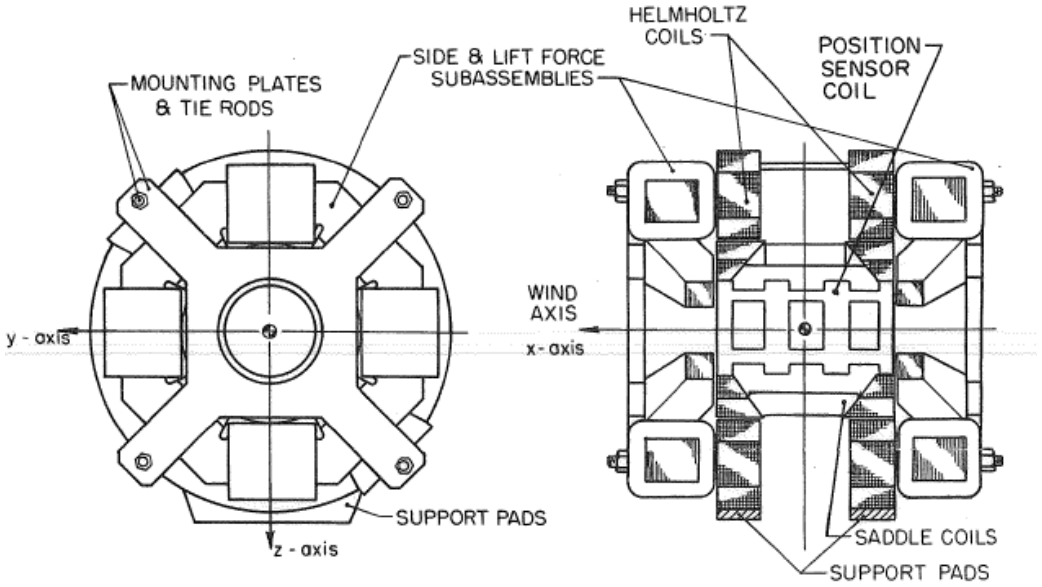

Fig. 3 Overall Configuration of the NASA/ODU 6-inch MSBS

A finite-element model of the NASA/ODU 6-inch MSBS has been developed using the AC/DC module of the COMSOL* multiphysics software package [8]. A few details of the model will be presented, with emphasis on the difficulties encountered and overcome, including:

- The 'as-built' geometry differs from the 'as-designed' (and documented) in some details, which are discussed by Driver [8].
- Point-by-point fields recovered from the COMSOL model can show some irregularity unless the local mesh is sufficiently refined. Smoothing by means of regression modeling is appropriate.
- The element count for a full 3D model is large, so half-models or quarter-models with symmetry assumptions may be used where appropriate.
- Material properties are poorly known, with modeling of laminated iron cores particularly challenging. The current model assumes linear (unsaturable) isotropic material, whereas the laminated sections are at least anisotropic, with some evidence of local saturation at the highest electromagnet current levels.

Work so far has been exclusively 'static', i.e., no time-varying currents. Figure 4 shows the baseline finite element model of the electromagnet assembly. A typical element count for the full model is 350,000. Coils are modeled as single conducting loops, with the overall current specified appropriately using the COMSOL multi-turn coil feature.

* COMSOL Multiphysics ™. The use of trademarks or names of manufacturers in this report is for accurate reporting and does not constitute an official endorsement, either expressed or implied, of such products or manufacturers by the National Aeronautics and Space Administration.

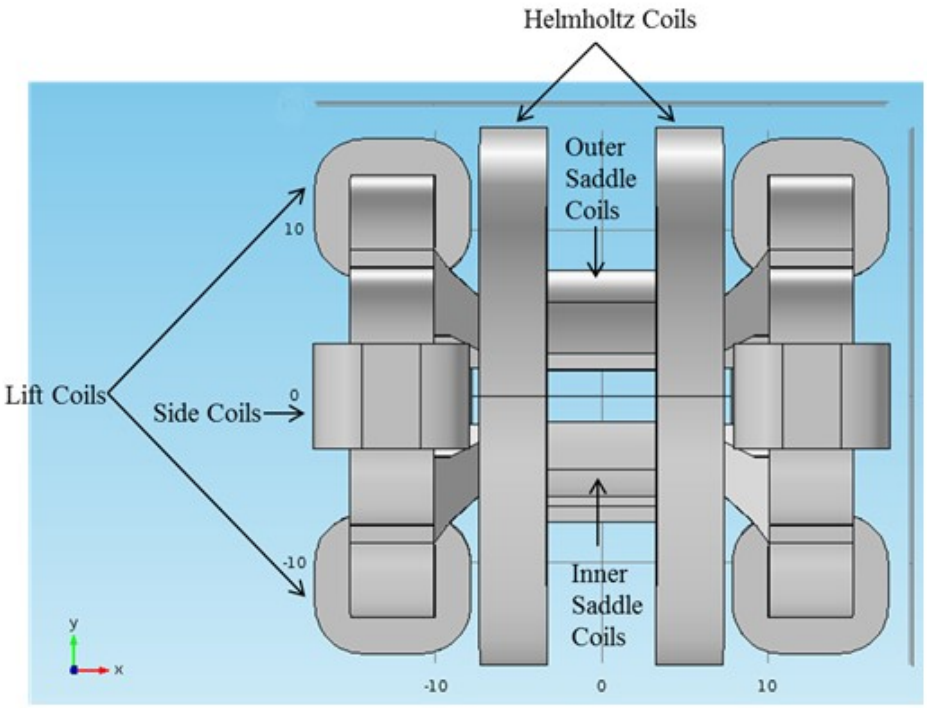

Fig. 4 COMSOL Model of the NASA/ODU/MIT 6-inch MSBS

V. Model Verification

Preliminary experimental verification of predicted field distributions has been carried out using a 3-axis gaussmeter probe (FW Bell 8000-series with Model 8030 gaussmeter) mounted on a 3-axis computer-controlled traverse, shown in Figure 5. Fields are automatically surveyed over a 3D grid with 125 points, 7 along the x-axis, with 5 each in y and z. A single coil set is energized for each survey, typically at 50 amps. With a few seconds pause at each measurement location a full survey takes 20-25 minutes. Field levels, field gradients, and second-order gradients can then be estimated by means of polynomial curve fitting of experimental data. Raw results may be corrected for errors in probe location and alignment using symmetry of the electromagnet array, but this process has not been completed at this time. Figure 6 shows a detail of one representative run, with the uncorrected polynomial regression fit below.

$$B_z = -0.015 - 0.121x + 0.001y + 0.002z \\ +0.009xy + 0.04xz + 0.014yz - 0.455x^2 + 0.009y^2 + 0.483z^2 \tag{21}$$

The primary field and gradient components are easy to identify, others are expected to be small largely due to symmetry in the y direction. Figure 7 shows all field components for the same run. Table 1 gives a summary of primary components derived from the field surveys. Comparison to the finite element predictions is moderate, as indicated in Table 2, with significant refinement possible.

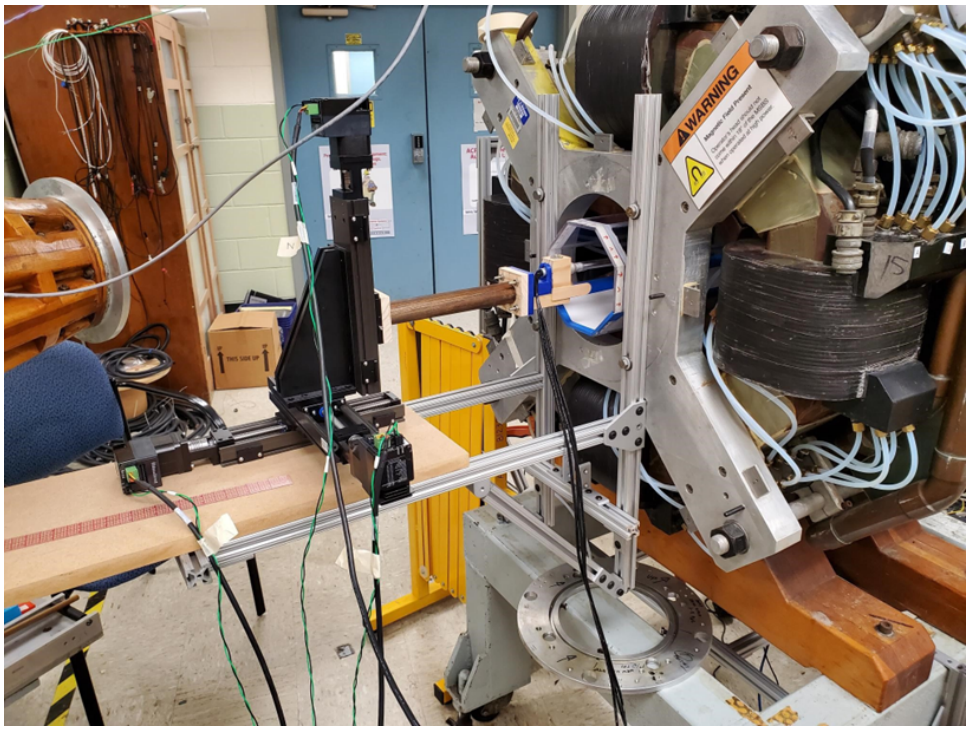

Fig. 5 – Field Survey Test Setup – upstream end of test section visible

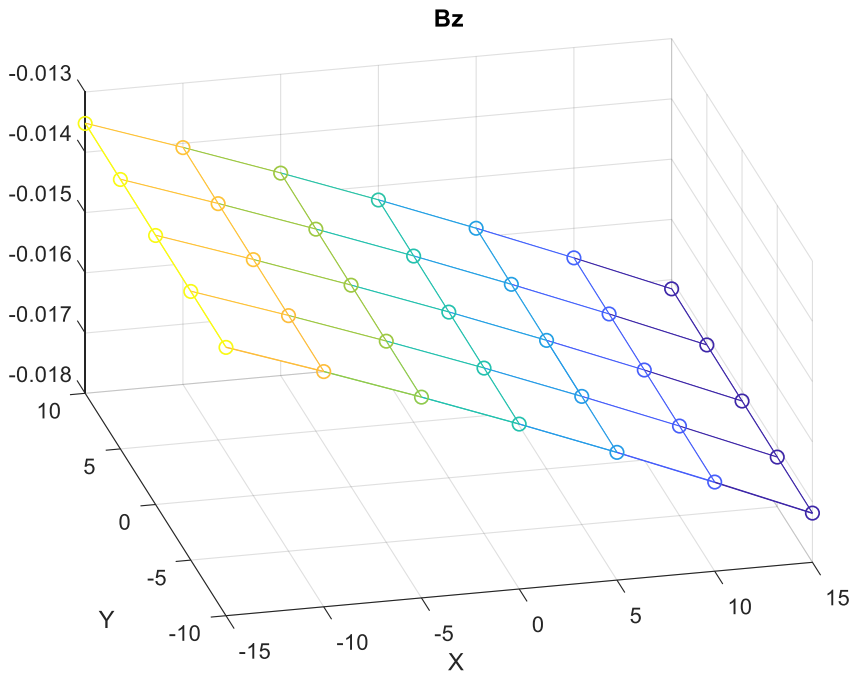

Fig. 6 – Vertical Field (B_z) on Horizontal Plane Through Tunnel Centroid

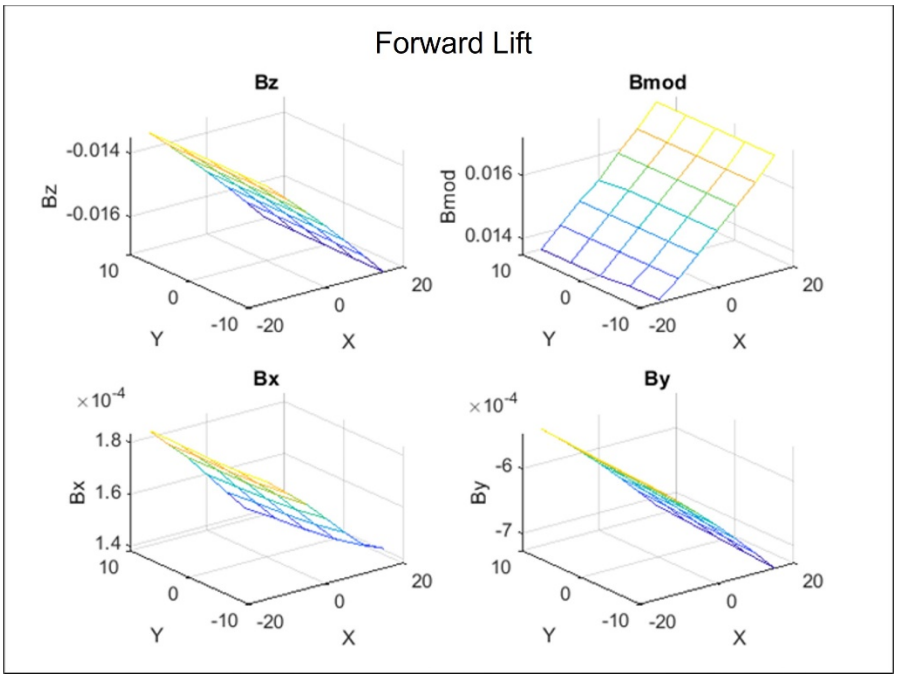

Fig. 7 – Example of Field Measurements (Forward Lift Coil Pair, 50A)

Table 1 – Primary Measured Field and Gradient Components from Each Coil Set at 50A
Units: Tesla, Tesla/m and Tesla/m²

Coil set	B_z	B_{xz}	B_{xxz}	B_{zzz}	
Forward lift	-0.015	-0.121	-0.943	0.966	
Aft lift	0.015	0.118	0.947	-0.93	
	B_{xx}	B_{yy}	B_{zz}	B_{xxx}	B_{yzz}
Helmholtz pair	-0.323	0.161	0.162	0.108	0.136
	B_{yz}	B_{zzz}			
Saddles	0.175	-0.18			

Table 2 – Primary Computed Field and Gradient Components from Each Coil Set at 50A
Units: Tesla, Tesla/m and Tesla/m²

Coil set	B_z	B_{xz}	B_{xxz}	B_{zzz}	
(Forward – aft) lift	-	0.283	-	-	
	B_{xx}	B_{yy}	B_{zz}	B_{xxx}	B_{yzz}
Helmholtz pair	-0.338	0.169	0.169	-	-
	B_{yz}	B_{zzz}			
Saddles	-	-			

VI. Model Analysis

An example case based on the NASA/ODU MSBS will illustrate how these equations of motion give rise to predicted modes which exhibit coupling between degrees of freedom. The equations of motion are then used as a framework for development of model-based feedback controllers.

The standard model core is a 19.05 mm (0.75 inch) diameter, 19.05 mm (0.75 inch) long cylindrical Neodymium-Iron-Boron (NdFeBo) permanent magnet core. The precise magnetization level is not known accurately but is taken

as 9.549×10^5 A/m (≡1.2 T, Grade N38) based on manufacturers information. The mass of the aerodynamic shell varies but a typical value is taken here as 25% of the core mass.

Drag is the primary aerodynamic force and is varied from zero (wind-off) to 1N, which corresponds to drag loads on Stardust-class capsules at dynamic pressures around 1kPa. Three levels of analysis are executed, with increasing fidelity, as described below. Results for case c) are presented in detail here.

a) Fields and field gradients only. This analysis isolates the most fundamental behavior, which will be relatively independent of specific electromagnet configurations.
b) Same as a) but with the B_{zz} field derived from an axial Helmholtz pair. If the required B_{zz} field was derived from a coil pair with its axis along z, the values of B_{xx} and B_{yy} would be 50% of B_{zz}. In the existing MSBS configuration, B_{zz} is derived (by necessity) from an axial gradient B_{xx}, so B_{xx}=2B_{zz} and B_{yy} and B_{zz} are equal.
c) Second order gradients, representative of the existing MSBS, are included.

For the case of zero drag force and 1N drag force, the predicted eigenvalues are shown in Table 3, along with the primary degrees of freedom involved in the eigenvector. Modes 1 and 2 are the "compass needle" terms as discussed earlier. Mode 3 is the primary coupling due to the B_{xz} field gradient. The lower frequency modes are easily stabilized/damped by the feedback controller. The compass needle terms are a concern since they lack damping. Introduction of damping by means of closing the control loops in the pitch and roll degrees of freedom may be necessary. It is also noted that the natural frequencies of the compass needle modes can be changed by adjustment of the alignment field (B_z). Perhaps most problematic is Mode 3, which is a fundamental coupling between axial and vertical translation as well as pitch rotation, due to the presence of the B_{xz} field gradient, which is turn opposes drag. The frequency rises as drag increases, so will present the biggest challenge as wind tunnel dynamic pressure (Mach number) increases. Mode 4 is an unstable dynamic with coupled roll and side motions that is relatively independent of the drag load. Mode 5 is an undamped oscillation that involves complex motion among the axes.

Table 3 – Eigenvalues for the Reference Case – Analytic Solution
Units: radians/sec

Mode #	Drag = 0 N	Drag = 1 N	Drag = 3 N	Degrees of Freedom
1	±216.9 j	±224.6 j	±240.9 j	θ
2	±234.0 j	±242.0 j	±257.3 j	ϕ
3	±11.26	±14.45	±33.84	x, z, θ
4	±5.96	±5.86	±5.69	y, ϕ
5	±12.52 j	±10.26 j	±4.78 j	complex motion

A. Comparison to Simulink* Models

In a related effort, a Simulink model of the MSBS has been developed to support control law design and analysis. The model can be automatically linearized about a chosen setpoint, with the resulting linear model used for design of the feedback controller via the LQG technique. Eigenvalues and mode shapes should match, thereby validating both approaches. Preliminary results for the refence case discussed above are shown in Table 4.

* Mathworks Inc. Matlab/Simulink ™ The use of trademarks or names of manufacturers in this report is for accurate reporting and does not constitute an official endorsement, either expressed or implied, of such products or manufacturers by the National Aeronautics and Space Administration.

Table 4 – Eigenvalues for the Reference Case – Derived from Simulation
Units: radians/sec

Mode #	Drag = 0 N	Drag = 1 N	Drag = 3 N	Degrees of Freedom
1	±215.4 j	±225.0 j	±246.0 j	θ
2	±232.3 j	±242.0 j	±260.4 j	ϕ
3	±12.1	±19.6	±47.5	x, z, θ
4	±5.0	±4.5	±3.6	y, ϕ
5	±12.8 j	±11.0 j	±5 j	complex motion

Some discrepancies are apparent, which arise at least in part to the differing numerical processes and treatment of the second order gradient terms. The Simulink model does not explicitly include second order gradient terms, instead it uses field and gradient terms derived from the experimental field survey grid and includes second order gradient effects through perturbation analysis. The analytical framework includes these terms explicitly, although some assertion of left-right symmetry is imposed during the analysis presented. Nevertheless, the agreement is satisfactory and supports the understanding of the fundamental behavior of the MSBS and extrapolation to higher dynamic pressures.

VII. Conclusions

The analytical framework presented gives insight into the fundamental dynamic behavior of MSBSs with high aerodynamic loads. For optimal performance, feedback control systems must incorporate knowledge of the fundamental couplings between degrees-of-freedom and the variations of this coupling with wind tunnel dynamic pressure. Agreement between analytic results and simulations seems acceptable. Further work to validate the predicted behavior against experimental results is required.

Appendix - Horizontal Magnetization Case

Careful inspection of the equations presented shows that some terms must be updated to accommodate the revised magnetization direction, whereas others are unchanged. Building from Equation (2), the modified terms are listed below for the case of magnetization along the traditional x axis (M_x).

$$F_x\ (\equiv \mathcal{X}) \approx Vol\ M_x B_{xx} \quad ; \quad F_y\ (\equiv \mathcal{Y}) \approx Vol\ M_x B_{xy} \quad ; \quad F_z\ (\equiv \mathcal{Z}) \approx Vol\ M_x B_{xz}$$

$$T_x\ (\equiv \mathcal{L}) \approx 0 \quad ; \quad T_y\ (\equiv \mathcal{M}) \approx -Vol\ M_x B_z \quad ; \quad T_z\ (\equiv \mathcal{N}) \approx Vol\ M_x B_y$$

$$\vec{M} = \begin{Bmatrix} M_x \\ 0 \\ 0 \end{Bmatrix}$$

$$\overrightarrow{F_c} \approx Vol\ M_x \begin{pmatrix} B_{xx} - 2B_{xz}\vartheta + 2B_{yz}\psi \\ B_{xy} + B_{xz}\phi - B_{yz}\vartheta + (B_{yy} - B_{xx})\psi \\ B_{xz} - B_{xy}\phi + (B_{xx} - B_{zz})\vartheta + B_{yz}\psi \end{pmatrix} \quad ; \quad \overrightarrow{T_c} \approx Vol\ M_x \begin{pmatrix} 0 \\ -B_z + B_y\phi - B_x\vartheta \\ B_y + B_z\phi - B_x\psi \end{pmatrix}$$

$$(\dot{\boldsymbol{X}}) = [W1] \begin{bmatrix} \mathcal{Z} & \mathcal{Z} & \mathcal{FP} & \mathcal{FA} \\ \mathcal{Z} & \mathcal{Z} & \mathcal{TP} & \mathcal{TA} \\ \mathcal{I} & \mathcal{Z} & \mathcal{Z} & \mathcal{Z} \\ \mathcal{Z} & \mathcal{I} & \mathcal{Z} & \mathcal{Z} \end{bmatrix} (\boldsymbol{X}) + \begin{bmatrix} K2_{xx,1} & \cdots & K2_{xx,n} \\ K2_{xy,1} & \cdots & K2_{xy,n} \\ K2_{xz,1} & \cdots & K2_{xz,n} \\ 0 & \cdots & 0 \\ -K1_{z,1} & \cdots & -K1_{z,n} \\ K1_{y,1} & \cdots & K1_{y,n} \\ 0 & \cdots & 0 \\ 0 & \cdots & 0 \\ 0 & \cdots & 0 \\ 0 & \ldots & 0 \\ 0 & \ldots & 0 \\ 0 & \ldots & 0 \end{bmatrix} \begin{pmatrix} I_1 \\ \vdots \\ I_n \end{pmatrix}$$

$$\mathcal{FP} = \begin{bmatrix} X_x & X_y & X_z \\ Y_x & Y_y & Y_z \\ Z_x & Z_y & Z_z \end{bmatrix} = Vol\ M_x \begin{bmatrix} B_{xx}|_x & B_{xx}|_y & B_{xx}|_z \\ B_{xy}|_x & B_{xy}|_y & B_{xy}|_z \\ B_{xz}|_x & B_{xz}|_y & B_{xz}|_z \end{bmatrix}$$

$$\mathcal{FA} = \begin{bmatrix} X_\phi & X_\vartheta & X_\psi \\ Y_\phi & Y_\vartheta & Y_\psi \\ Z_\phi & Z_\vartheta & Z_\psi \end{bmatrix} = Vol\ M_x \begin{bmatrix} 0 & -2B_{xz} & 2B_{xy} \\ B_{xz} & -B_{yz} & (B_{yy} - B_{xx}) \\ -B_{xy} & (B_{xx} - B_{zz}) & B_{yz} \end{bmatrix}$$

$$\mathcal{TP} = \begin{bmatrix} \mathcal{L}_x & \mathcal{L}_y & \mathcal{L}_z \\ \mathcal{M}_x & \mathcal{M}_y & \mathcal{M}_z \\ \mathcal{N}_x & \mathcal{N}_y & \mathcal{N}_z \end{bmatrix} = Vol\ M_x \begin{bmatrix} 0 & 0 & 0 \\ -B_{xz} & -B_{yz} & -B_{zz} \\ B_{xy} & B_{yy} & B_{yz} \end{bmatrix}$$

$$\mathcal{TA} = \begin{bmatrix} \mathcal{L}_\phi & \mathcal{L}_\vartheta & \mathcal{L}_\psi \\ \mathcal{M}_\phi & \mathcal{M}_\vartheta & \mathcal{M}_\psi \\ \mathcal{N}_\phi & \mathcal{N}_\vartheta & \mathcal{N}_\psi \end{bmatrix} = Vol\ M_x \begin{bmatrix} 0 & 0 & 0 \\ B_y & -B_x & 0 \\ B_z & 0 & -B_x \end{bmatrix}$$

$$\therefore \ \overline{B_{xx}} = \frac{D}{Vol\ M_x} \quad ; \quad \overline{B_{xy}} = \frac{-S}{Vol\ M_x} \quad ; \quad \overline{B_{xz}} = \frac{L - m_c g}{Vol\ M_x}$$

Acknowledgments

This work was supported by NASA Langley Research Center, Entry Systems Modeling Project, part of NASA's Game Changing Technology Program, activity NNL09AA00A #201001 awarded to the National Institute of Aerospace. The NASA monitor is Mark Schoenenberger, Atmospheric Flight and Entry Systems Branch.

References

[1] Driver, D., "Electromagnetic Modeling of a Wind Tunnel Magnetic Suspension and Balance System," Master of Science Thesis, Department of Mechanical and Aerospace Engineering, Old Dominion University, May 2022

[2] Covert, E.E.; Finston, M.; Vlajinac, M.; Stephens, T., "Magnetic Balance and Suspension Systems for Use with Wind Tunnels," *Progress in Aerospace Sciences*, Volume 14, 1973

[3] Goodyer, M. J., "Roll Control Techniques on Magnetic Suspension Systems," *Aeronautical Quarterly*, vol. 18, 1967, Pt. 1, pp. 22-42

[4] Groom, N.J., "Analytical model of a five degree of freedom magnetic suspension and positioning system," NASA TM-100671, March 1989

[5] Groom, N.J.; Britcher, C.P., "Open-loop characteristics of magnetic suspension systems using electromagnets mounted in a planar array," NASA TM-3229, November 1992

[6] Groom, N.J., "Expanded Equations for Torque and Force on a Cylindrical Permanent Magnet Core in a Large-Gap Magnetic Suspension System," NASA TP-3638, February 1997

[7] Schoenenberger, M.., "Static and Dynamic Testing of Blunt Bodies in a Subsonic Magnetic Suspension Wind Tunnel," *16th International Planetary Probes Workshop*, July 2019

[8] Stephens, T., "Design, Construction and Evaluation of a Magnetic Suspension and Balance System for Wind Tunnels," NASA CR-66903, November 1969